

# Synthesis and Evaluation of Optical Properties of the New Organic Compound Containing 9-Methylcarbazole and Cyanoacrylic Acid

Marzieh Rabiei<sup>#,1</sup>, Ali Hamidi<sup>\*</sup>

<sup>#</sup>Advanced Materials Research Center, Materials Engineering Department, Najafabad Branch, Islamic Azad University, Najafabad, 8514143131, Iran

<sup>\*</sup>Faculty of Technology, Linnaeus University, Vaxjo 35195, Sweden

<sup>1</sup>Corresponding author

**Abstract**— Organic materials that exhibit fluorescence are an attractive class of functional materials and optical properties that have witnessed a booming development in recent years. The design of new system with Donor-Acceptor properties is great interest for the construction of photophysical properties. D-A dye based on Indoline involved of 9-Methylcarbazole as a donor and cyanoacrylic acid as an acceptor synthesized via ideal process of carbazole as a primary substance. Synthesized compound was characterized by thin layer chromatography (TLC), differential scanning calorimetry (DSC), thermal Gravimeter analysis (TGA), fourier transform infrared spectroscopy (FTIR), <sup>1</sup>H-nuclear magnetic resonance (<sup>1</sup>HNMR), <sup>13</sup>C-NMR, liquid chromatography, ultraviolet-visible spectroscopy in solutions and solid film. Photoluminescence quantum yields (PLQYs) of 2-11% in solution and 17% in non-doped solid film reported. To get further insight into the molecular structure of dye, their geometry and energies of HOMO and LUMO were optimized by density functional theory (DFT) calculation at the B3LYP/6-31G(d) level with Gaussian software 09. The melting point of dye reported 142 °C and the synthesized compound absorbs electromagnetic radiation in the range of 424-431 nm in solutions and emit solid film exhibited fluorescence in 541 nm. According to the results of investigations, compound was aggregation induced emission (AIE) and the ionization potentials of the synthesized dye was found to 5.89 eV.

**Keywords**— Indoline, Carbazole, Electrochemical properties, Optical properties, Cyanoacrylic acid

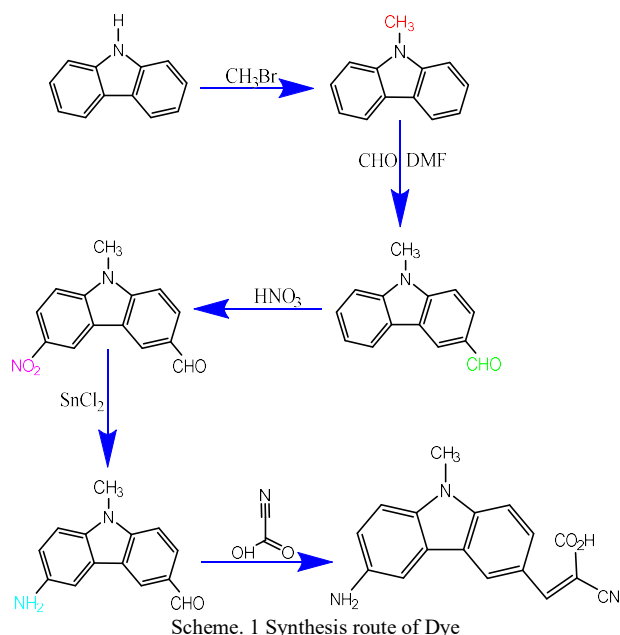
## I. INTRODUCTION

Over the past few decades, the synthesis and investigation of  $\pi$ -conjugated organic materials has drawn considerable amount of research attention owing to their possible applications in the field of organic optoelectronics [1]. Presently, conjugated compounds with electron-donating (D) and electron-accepting (A) units are special attention because of their applicability in optoelectronic and electronic devices, such as organic light emitting diodes (OLEDs) [2], solar cells [3] and chemical sensors [4]. Compounds having donor and acceptor moieties often exhibit narrow energy gaps resulting from intramolecular charge transfer (ICT) [5].

Specially, the design and development of donor-acceptor  $\pi$ -conjugated dyes with both electron donating (D) and electron-accepting (A) groups, which possess high molar extinction coefficients, are expected to be one of the most promising organicsensitizers [6,7,8,9,10,11,12,13].

Organic compounds containing cyanoacrylic acid have been extensively studied as organic dyes in dye-sensitized solar cells due to their power conversion efficiency, ease of preparation, high structural flexibility, high extinction coefficients in the visible region and relatively low cost [14,15,16,17,18]. Totally the structure of Indoline considered very much, because it has suitable stability, high conversion efficiency and ease synthesis.

There are several researches on cyanoacrylic acid as an acceptor, for example Paul et al synthesized new dye involved of cyanoacrylic acid as an acceptor for using in solar cells [19]. Dehno Khalaji et al used cyanoacrylic acid as an acceptor in prepare of dyes [20] and Linxi et al designed structure with cyanoacrylic acid as an acceptor [21]. Furthermore materials with carbazole display stronger brightness and higher stability [22]. Until now, many kinds of organic compounds containing cyanoacrylic acid group as an acceptor have been developed, such as coumarin, indoline, triphenylamine and rhodanine [9-13], but there is rare report on relation between carbazole moieties and cyanoacrylic. Nevertheless, the necessity of design and synthesis of new donor-acceptor materials with improved optical, photophysical and thermal properties is still an urgent topic. Therefore, in the strategy of this study, we have synthesized and investigated optical properties of new organic compound without metal with carbazole as a primary material with substitution methyl on nitrogen heteroatom containing cyanoacrylic acid and 9-Methylcarbazole (Scheme 1).



## II. METHODS

### II.1 Materials and Instrumentation

All materials of consumption are Merck Co. The FTIR spectra were recorded on a PerkinElmer Spectrum GX II FT-IR One spectrophotometer on a KBr disc. The  $^1\text{H}$ -NMR and  $^{13}\text{C}$ -NMR spectra (chemical shifts are given as  $\delta$  in ppm) were recorded on a Bruker DRX AVANCE spectrometer operating at 500 MHz. The elemental analysis CHNS was determined on a Costech instruments (Elemental Combustion System 4010). Differential scanning calorimetry (DSC) measurements were carried out using a DSC (DSC 214 Polyma NETZSCH) under nitrogen environment. Cyclic voltammetry measurements were performed on a PGSTAT 302, electrochemical experiments were carried out at room temperature using a three electrode cells consisting of a platinum coil as counter electrode, a glassy carbon working electrode, and a silver wire as reference electrode. 0.1 M solution of tetrabutylammonium hexafluorophosphate ( $n\text{-Bu}_4\text{NPF}_6$ ) was used as supporting electrolyte at a scan rate of 100 mVs $^{-1}$ . For the measurements, silver reference electrode was calibrated against Ferrocene/Ferrocenium ( $\text{Fc}/\text{Fc}^+$ ) redox couple as an internal standard [23].

The UV-Vis absorption spectra were recorded on a Cecil 9200 double beam spectrophotometer and the fluorescence spectra were taken on a Perkin and Elmer LS50B spectrofluorimeter with both excitation and emission slits set at 10 nm and controlled by a personal computer data processing unit. To record photoluminescence decay curves dependencies on laser flux, with Pico Quant LDH-D-C-375 laser with wavelength equals 373 nm as the excitation source were used and the ionization potential (IP) of the vacuum deposited films was obtained using photoelectron emission spectrometry in air [24,25].

### II. 2 Synthesis

#### II.2.1 9-methyl-9H-carbazole (1)

2 mol of carbazole and 18 ml of DMF stirred under the condenser and prepared clear suspension via heating in bath oil. 1 and 1.5 mol bromomethyl and potassium tert butoxide added to suspension respectively and stirred and after 15 hours crystals were formed and after filtration the yellow product dried via chromatography and purified with ethyl acetate/hexane.

MP=98°C; FTIR (KBr) ( $\text{Cm}^{-1}$ ): 3321: C-H str Aromatic, 1657, 1470: C=C str, 1298: C-N str;  $^1\text{H}$ NMR ( $\text{CDCl}_3$ ),  $\delta$  (ppm): 2.37 (s, 3H,  $\text{CH}_3$ ), 7.38-7.47 (d, 2H), 7.57-7.59 (t, 2H), 7.73-7.76 (t, 2H), 8.10-8.12 (d, 2H); Elem. Anal. Calcd. for  $\text{C}_{13}\text{H}_{11}\text{N}$ : C, 87.04%; H, 5.69%; N, 7.25%. Found: C, 87.03%; H, 5.71%; N, 7.26%.

#### II.2.2 3-formyl-9-methyl-9H-carbazole (2)

2 mol of (1) in 15 ml of DMF stirred and after 15 minutes added 1 mol of phosphoryl chloride to the reaction and stirred in 4 °C and arrived to room temperature very slowly around 3 hours. Final product filtrated after the using water and produced yellow material after the purification in ethyl acetate/hexane.

MP=112.3°C; FTIR (KBr) ( $\text{Cm}^{-1}$ ): 2863: C-H str. Ald, 1721: C=O str, 1649, 1466: C=C str, 1288: C-N str;  $^1\text{H}$ -NMR ( $\text{CDCl}_3$ ),  $\delta$  (ppm): 2.54 (s, 3H,  $\text{CH}_3$ ), 7.04-7.07 (d, 2H), 7.09-7.12 (t, 1H), 7.16-7.17 (t, 1H), 7.33-7.35 (d, 1H), 7.40-7.42 (t, 1H), 7.45-7.49 (s, 1H), 8.67-8.69 (s, 1H, COH); Elem. Anal. Calcd. for  $\text{C}_{14}\text{H}_{11}\text{NO}$ : C, 80.38%; H, 5.26%; N, 6.69%. Found: C, 80%.39; H, 5.26%; N, 6.68%.

#### II.2.3 3-formyl-7-Nitro-9-methyl-9H-carbazole (3)

0.2 mol of (2) stirred in 40 gr of acid acetic and reaction was cold until room temperature (RT) and added 5 gr of nitric acid very slowly. The temperature of reaction increased to 90 °C for 3 hours and final product filtrated after the using water/acetic and produced yellow material after the purification in ethyl acetate/hexane.

MP=116.9 °C; FTIR (KBr) ( $\text{Cm}^{-1}$ ): 1;554, 1348:  $\text{NO}_2$  str, 1758: C=O str., 1630, 16456: C=C str, 1278: C-N str;  $^1\text{H}$ -NMR ( $\text{CDCl}_3$ ),  $\delta$  (ppm): 1.93 (s, 3H,  $\text{CH}_3$ ), 6.64-6.66 (d, 2H), 6.71-6.73 (d, 1H), 6.76-6.78 (d, 1H), 6.83-6.86 (s, 1H), 7.16-7.19 (s, 1H), 8.55 (s, 1H, COH); Elem. Anal. Calcd. for  $\text{C}_{14}\text{H}_{10}\text{N}_2\text{O}_3$ : C, 65.62%; H, 3.93%; N, 11.02%. Found: C, 65.63%; H, 3.92%; N, 11.03%.

#### II.2.4 3-formyl-7-Amino-9-methyl-9H-carbazole (4)

1 gr of (3) stirred with 3 gr of Tin(II) chloride and 10 ml isopropyl alcohol and 5 ml hydrochloric acid stirred respectively for 3 hours, final product filtrated after the using water/acetic and produced yellow material after the purification in ethyl acetate/hexane.

MP=129.14 °C; FTIR (KBr) ( $\text{Cm}^{-1}$ ): 3531: NH str., 1672:

C=O str, 1588, 1435: C=C str, 1259: C-N str;  $^1\text{H-NMR}$  ( $\text{CDCl}_3$ ),  $\delta$  (ppm): 2.34 (s, 3H, CH<sub>3</sub>), 4.24-4.28 (2H, NH<sub>2</sub>), 6.60-6.62 (d, 2H), 7.43-7.44 (d, 1H), 7.45-7.47 (d, 1H), 8.12 (s, 1H), 8.24 (s, 1H), 9.25 (s, 1H, COH); Elem. Anal. Calcd. for  $\text{C}_{14}\text{H}_{12}\text{N}_2\text{O}$ : C, 75%; H, 5.35%; N, 12.5%. Found: C, 75.02%; H, 5.36%; N, 12.48%.

### II.2.5 Dye

10 mmol of (4) and 50 ml acetonitrile and 15 mmol cyanoacetic and 50 ml pyridine stirred respectively for 10 hours, after cooling until room temperature and filtration and purification in ethyl acetate/hexane, the dye dried and synthesized. The yield of reactions for (1), (2), (3), (4) and dye were 78%, 87%, 84%, 81% and 84% tandemly.

MP=127.13 °C; FTIR (KBr) ( $\text{Cm}^{-1}$ ): 1676: C=O str, 1581, 1442: C=C str, 1244: C-N str;  $^1\text{H-NMR}$  ( $\text{CDCl}_3$ ),  $\delta$  (ppm): 2.27 (s, 3H, CH<sub>3</sub>), 4.33-4.38 (2H, NH<sub>2</sub>), 6.77-6.79 (d, 2H), 7.21-7.24 (d, 1H), 7.35-7.37 (d, 1H), 7.62 (s, 1H), 7.94 (s, 1H), 10.18 (s, 1H, COH); Elem. Anal. Calcd. for  $\text{C}_{17}\text{H}_{13}\text{N}_3\text{O}_2$ : C, 70.10%; H, 4.46%; N, 14.43%. Found: C, 70.09%; H, 4.47%; N, 14.44%.

## III. RESULTS

### III.1 Geometries and frontier orbitals

DFT/TDDFT calculations were carried out with B3LYP hybrid functional combined with 6-31G(d) basis set. For investigated compounds ground state geometries were optimized with no symmetry constraints to a local minimum, which was followed by frequency calculations.

In all cases no imaginary frequencies were found. All calculations in this work were conducted with polarizable continuum model (PCM) using dichloromethane as solvent as implemented in Gaussian 09 software [26]. Input files and molecular orbital plots were prepared with Gabedit 2.4.7 software [27]. The theoretical geometries and the distribution of HOMO and LUMO of synthesized dye are presented in Figure 1.

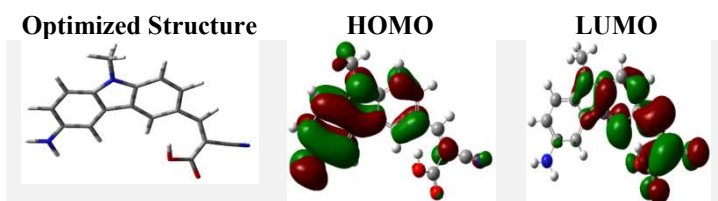


Fig. 1 Shape of frontier orbitals of dye, calculated at B3LYP/6-31G(d)/PCM(DCM) and isovalue is equal to  $0.03 \text{ e}^-/\text{au}^3$

### III.2 Thermal properties

Thermal properties of the synthesized dye was estimated by Differential Scanning Calorimetry (DSC) and Thermal Gravimetric Analysis (TGA) under nitrogen environment at a heating rate of  $10^\circ\text{C}/\text{min}$  and the curves brought in Figure 2.

In the TGA measurements, the dye exhibited  $\sim 7\%$  mass loss temperature in the range  $230\text{--}260^\circ\text{C}$ . The shape of TGA curve and very low quantity of residue at the end of experiment allows to assume that during heating carbazole was sublimated (Figure 2). Dye was isolated after the synthesis as crystalline substances and their first DSC heating scans exposed endothermic melting signal ( $T_m$ ). The glass transition temperature of dye was found to be close to  $90^\circ\text{C}$  and DSC heating scan it showed only sharp endothermic signal at  $142^\circ\text{C}$  due to sublimation.

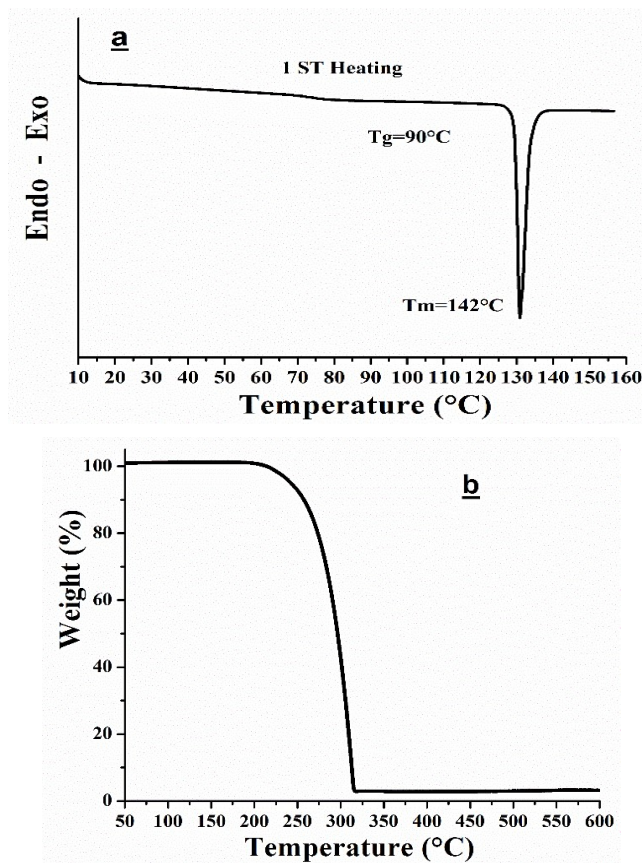


Fig. 2 a) DSC curve and b) TGA curve of dye

### III.3 Electrochemistry

Electrochemical property of investigated dye was determined using cyclic voltammetry (CV). Voltammograms of investigated dye is presented in Figure 3, while resulting data is presented in Table 1. Onset of oxidation of described molecule is located at  $0.88 \text{ V}$  and characterized by reversible oxidation peak, indicating that stable radical cations are formed during electrochemical oxidation. Dye displayed two oxidation peak, which can be assigned to oxidation of electron donating carbazole moieties and  $\text{NH}_2$ . According to the method reported by Forrest et al.[28], ionization energy values ( $\text{IP}_{\text{CV}}$ ) value was calculated using the equation  $\text{IP}_{\text{CV}} = -(1.4 \times 10^6 \times E_{\text{onset}}^{\text{ox}} \text{ vs Fc/V}) - 4.6 \text{ eV}$ . The value of  $\text{IP}_{\text{CV}}$  is given in Table 1.

Ionization potentials ( $\text{IP}_{\text{EP}}$ ) of the solid layer of dye was



estimated by photoelectron emission spectrometry.

Photoelectron emission spectra is shown in Figure 4. These values were compared with vertical ionization potentials, theoretically calculated in the framework of DFT B3LYP/6-31G(d) approach (Table 1). The trend of the ionization potential of CV was found to be close to those estimated by photoelectron emission spectrometry. The lowest value of theoretical vertical IP level was observed for dye, while the derivatives exhibit higher values of IP. It has to be mentioned that the trend of IP is not strictly consistent with the HOMO energy levels. The main reason is that the B3LYP basis set functional cannot predict orbital energies accurately [29].

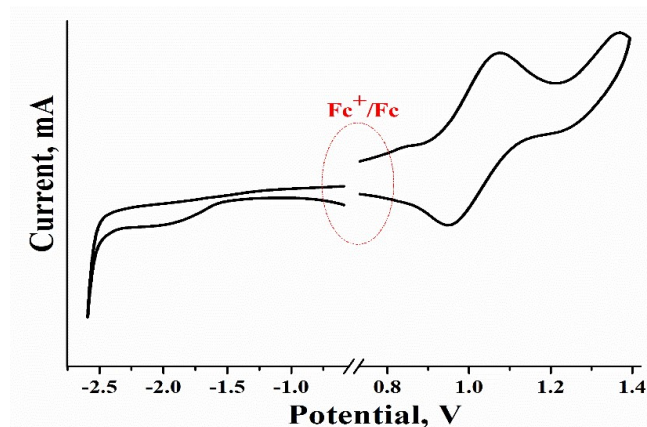


Fig. 3 Cyclic voltammograms of dilute solution of dye in dichloromethane (DCM) at sweep rate of 100 mV/s

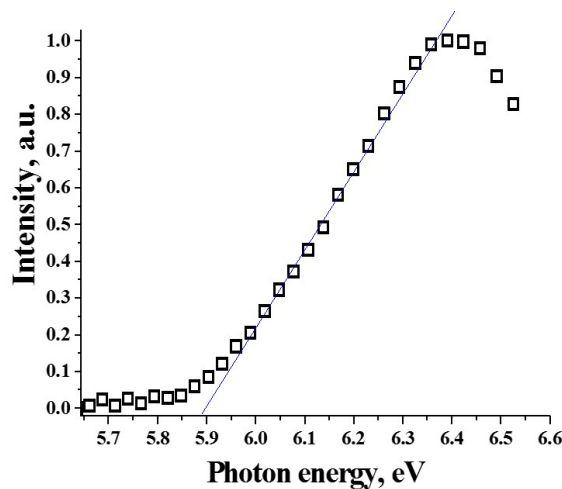


Fig. 4 Photoelectron emission spectra of the solid sample

TABLE I Electrochemical and electronic properties of investigated dye

$E_{\text{onset}}^{\text{ox}}$ (V)	$E_{\text{onset}}^{\text{red}}$ (V)	$E_{\text{g}}^{\text{opt}}$ (eV)	$\text{IP}_{\text{CV}}$ (eV)	HOMO (eV)	LUMO (eV)	$\text{EA}_{\text{CV}}$ (eV)	$\text{IP}_{\text{V}}$ (eV)	$\text{IP}_{\text{PE}}$ (eV)
0.88	-1.52	2.49	5.83	5.41	2.28	2.92	4.27	5.89

$E_{\text{ox}}$ : Potential of onset of oxidation and estimated from CV

$E_{\text{red}}$ : Potential of onset of oxidation and estimated from CV

$E_{\text{g}}^{\text{opt}}$ : Calculated with the relation  $1239.75/\lambda$  of UV spectra (in Toluene)

$\text{IP}_{\text{CV}}$  = Ionization potentials calculated with the relation  $|(1.4 \times 10^{-5} \times E_{\text{ox}} \text{ vs Fc/V}) - 4.6|$  eV [30].

HOMO: Energy level Estimated by DFT

LUMO: Energy level Estimated by DFT

$\text{EA}_{\text{CV}}$ : Calculated with the relation  $\text{EA}_{\text{CV}} = -(\text{IP}_{\text{CV}} - E_{\text{g}}^{\text{opt}})$

$\text{IP}_{\text{V}}$ : Vertical ionization potentials, calculated at the B3LYP/6-31G(d)

$\text{IP}_{\text{PE}}$ : Ionization potentials estimated by electron photoemission

#### III.4 UV-vis and fluorescence properties

Absorption and PL (photoluminescence) spectra of the dilute solutions of dye (0.00001 M) and solid film are shown in Figure 5 and wavelength ranges of the main absorption bands and fluorescence were shown in Table 2.

A shape and a wavelength range of the main absorption bands only slightly changes in this series of dye and presented in Table 2. Furthermore, Characteristic peak at ~400-540 nm is observed. Moreover, lower intensity band is located at longer wavelength range 485 until 510 nm. The difference in wavelength of emission between spectra of Toluene and Chloroform is equal to 0.22 eV. This effect is suggested an increase in the conjugation level of the  $\pi$  orbitals [31]. The different effect of solvents Toluene and Chloroform on the emission spectra of dye was studied and the wavelength of maximum intensities exhibited bathochromic leads to the strong red shift from the lowest polarity (Toluene, according to the index polarity of Table 2) to highest polarity (Chloroform) environments, compared to that of the individual donor and acceptor emission spectra and PL spectra move to longer wavelengths with increasing solvent polarity, showing a strong positive solvatochromism and as displayed previously in other donor-acceptor type of molecules [32,33,34]. Actually red shift of Chloroform solution demonstrated that the related with constant vibronic structure insensitive to the changing of environmental polarity [35,36].

Therewith, increases of solvents polarity observed charge transfer energy red shifted and investigated in less local excited state (LES) parameter and higher energy difference between charge transfer axial and charge transfer equatorial [37,38,39] and indicates that existed certain degree of charge transfer character with a large dipole moment which is derived from low lying singlet excited state [40,41]. Furthermore, for the emission spectra of dye in Toluene observed two peaks (Figure 5) that it is related to vibronic structure [42]. Emitted green light with maximum wavelength at 541 nm observed in solid state film and in the emission spectra of the solid state film broad band in the range of ~418-780 nm appears. Origin of this band lies in dimers formed by  $\pi$ -stacking between

carbazole moieties in the solid state in excited state, called excimer, as described by other authors [43]. According to the Table 2 large stokes shifts observed for dye in Chloroform ( $5567\text{cm}^{-1}$ ) can apparently be explained by the large changes in geometry between the excited and ground states and the intramolecular charge transfer (ICT) from carbazole to cyanoacrylic acid moieties. Expansion of  $\pi$ -conjugated systems in dye in polar solutions such as chloroform leads to increase of relaxation time and results in higher stokes shifts of  $4693$  to  $5567\text{ cm}^{-1}$  (THF and Chloroform), respectively. In this case, methyl group attached at the positions of carbazole moiety not only expand the conjugation of the  $\pi$ -electron system but also increase the dipole moment of the molecule [44].

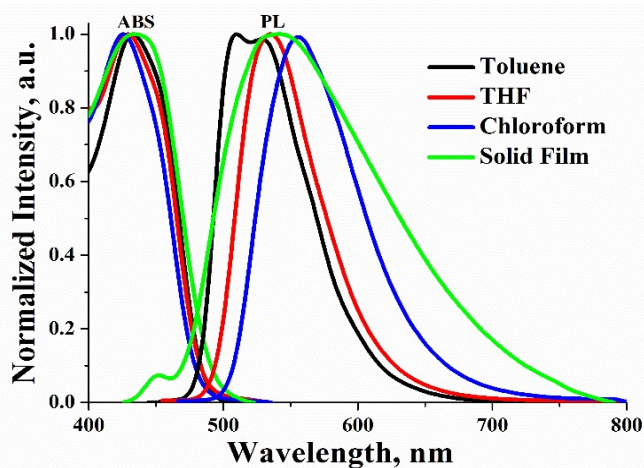


Fig. 5 ABS spectra and PL spectra of dye dissolved in different solutions and solid film

TABLE II Spectroscopic properties of the studied dye determined in solutions and solid film

Parameter	$\lambda_{\text{Max}}^{\text{ABS}}$ (nm)	$\lambda_{\text{Max}}^{\text{Em}}$ (nm)	Polarity Index	$\Delta(\text{cm}^{-1})$	PLQY (%)	$S_1$ (eV)	Polarity Index
Toluene	431	507	2.4	3478	2	-	2.4
THF	427	534	4.0	4693	8	2.65	4.0
Chloroform	424	555	4.1	5567	11	-	4.1
Solid Film	434	541	-	3587	17	2.54	-

$\Delta$ : Minimum Stokes shift

PLQY: Quantum efficiency

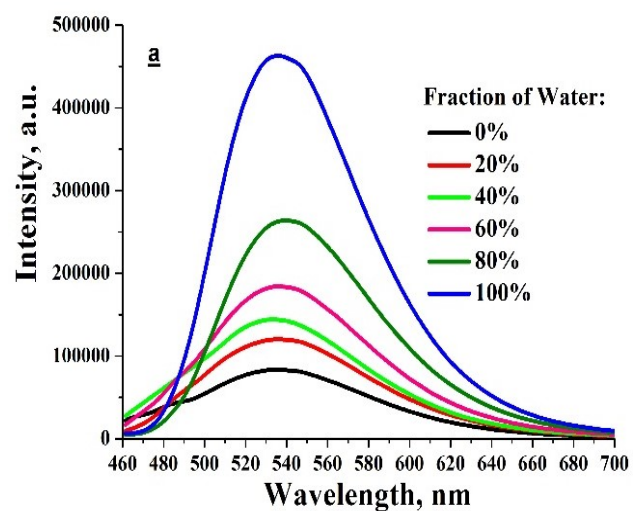
To assessment experimental quantity of singlet energy ( $S_1$ ), photoluminescence spectra were recorded at low temperature (80 K) in THF solution and cryostat system of solid film (Figure 7). Singlet energy levels of the dye were found to be comparable and therefore values reported 2.65 and 2.54 eV in THF and solid film respectively (Table 2), as well as we didn't observe red shifted spectra and phosphorescence phenomena and the spectra was similar to PL spectra in room temperature.

The similar trend is observed for the values of photoluminescence quantum yield (PLQY) of the studied dye.

With the increasing number of index polarity, PLQY increases from 2% to 11% and low PLQY is probably caused by vibrations of methyl group [45]. The PLQY in the solid film of investigated dye is within the value of 17%. Note that this means that molecules enhance their luminescence efficiency in solid state, while PLQY for dye in solutions decreases. Moreover, the increase of PLQY is caused by reduction of molecular vibration in solid state, therefore we investigated Aggregation Induced Emission (AIE) phenomena for dye and the corresponding results are presented in Figure 6.

To examine whether for dye is active and qualified of AIE and as well as dye is miscible in THF and Water at room temperature, we accomplished PL spectra analysis on dye in the THF/Water mixtures with water fractions ranging from 0 until 100 percent of volume (Figure 6).

In Fig 6, exhibited a very weakly green emission with a maximum wavelength of 534 nm at 40 % of water fraction, although PL intensities increased suddenly of aggregates in 80% and finally 100% of water fractions. Moreover, wavelength of PL spectra was not bathochromically shifted impressively, and simultaneously there is a broad spectral shape of the emission that estimated the violent bright PL emanates from the Intramolecular Charge Transfer (ICT) excited state between the 9-Methylcarbazole as a donor and cyanoacrylic acid as an acceptor unit. In water fraction values of 0% for dye, equivalent to enhancement behavior was not observed Aggregation Induced Emission Enhancement (AIEE) in THF/Water mixtures and we encountered with AIE owing to structural difference of dye and restriction of intermolecular motion and finitude the internal rotations in the acceptor unit (cyanoacrylic acid). Hence, the observed AIE activities that it is the first of all the same mechanism and ascribed to aggregation induced restriction of suitable changes in the donor unit and the rotation around the single bond between the units of donor and acceptor [46,47,48].



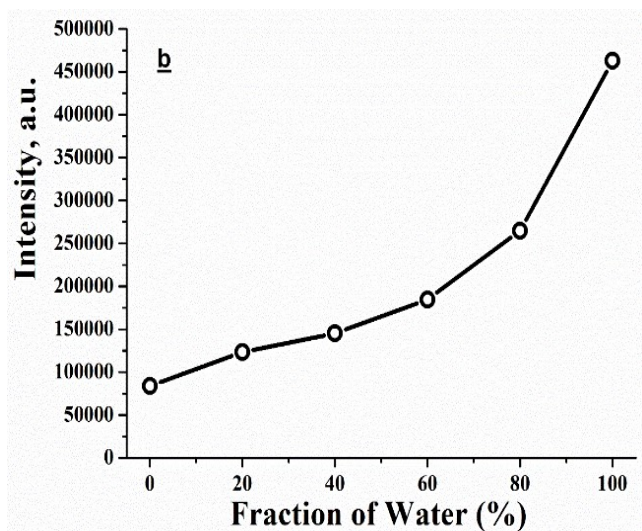


Fig. 6

- a) PL spectra of dye in the THF/Water mixtures  
 b) The inset plot of dye indicated the relationship between PL maximum intensities and water volume fraction in THF/Water mixtures

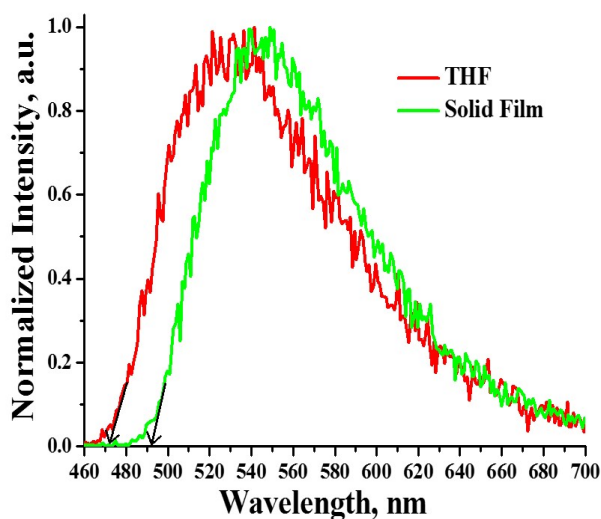
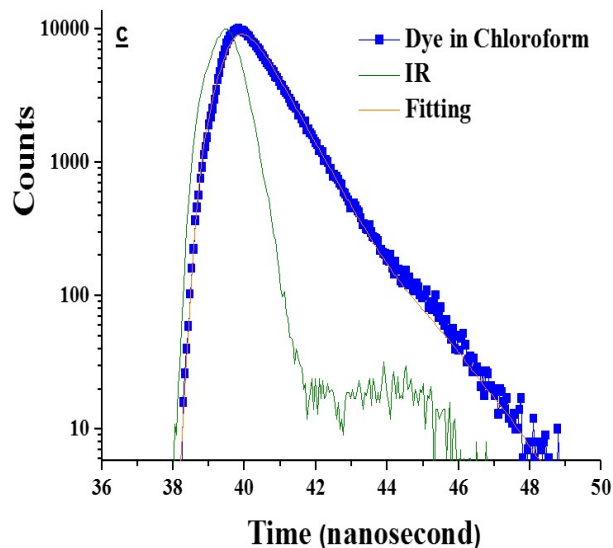
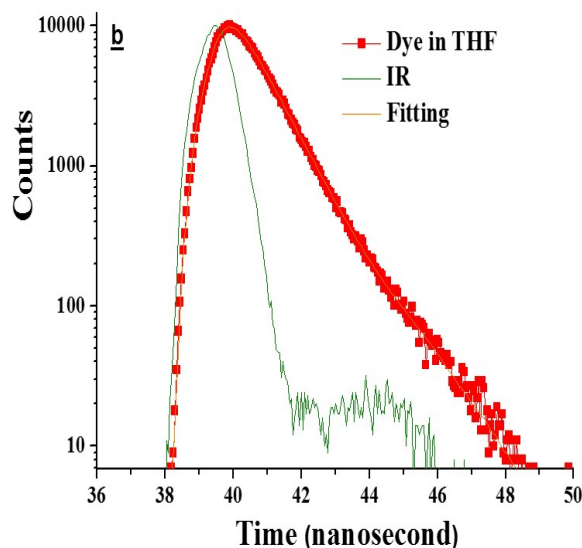
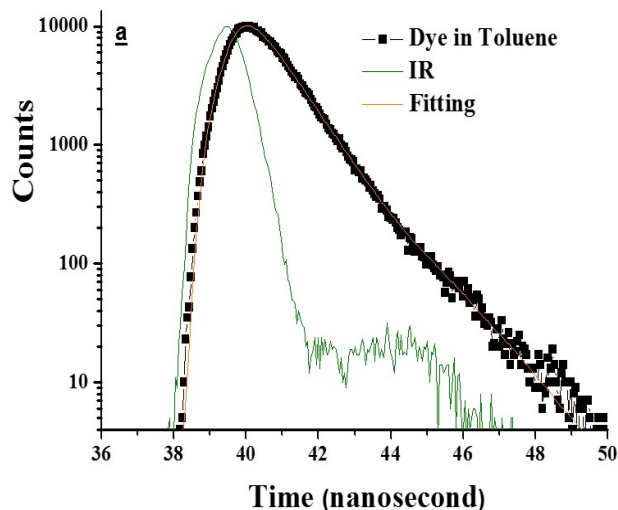


Fig. 7 PL spectra of dye in THF and neat film recorded at 80K

### III.5 Evaluation of PL decays

Fluorescence decay profiles of solutions and solid films were recorded with using of a single photon counting spectrofluorimeter. PL decays were monitored at the corresponding emission maximum of the dye and software experimental fluorescence allowed the fitting of value the decay spectra 1 until 1.2. According to the Figure 8 and Table 3, appearing of the slower decay for dye in solutions, occurred in the range of 0.81-0.91 ns and long decay time (9.11 ns) for solid state that the reasons are associated with the weak intermolecular interactions or crystalline aggregate formations in the neat films [49].





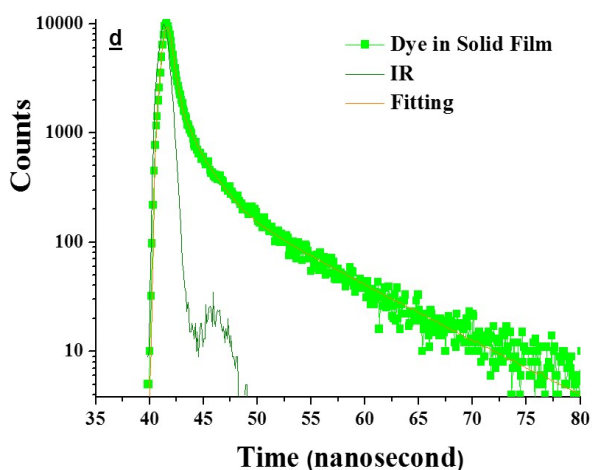


Fig. 8 Transient PL decay curves of dye in (a) Toluene (b) THF (c) Chloroform (d) neat Solid Film at room temperature

TABLE III Life-Time fitting data of dye in solutions and Solid Film

Dye				
Parameters	Toluene	THF	Chloroform	Solid Film
$\tau_1$ , ns	0.91	0.86	0.81	0.19
$\tau_2$ , ns	-	-	-	2.02
$\tau_3$ , ns	-	-	-	9.11
$\chi^2$	1.145	1.117	1.119	1.062

#### IV. CONCLUSIONS

In this study, a series of new dye based on Idoline synthesized via carbazole as a primary material, we considered carbazol as a donor and cyanoacrylic acid as an acceptor. Dye prepared by knoevenagel reaction and after the purification used several analysis instruments such as FTIR,  $^1\text{H}$ NMR and DSC/TGA. According to the optical properties of dye absorption spectra were in the range of 424-431 nm in solutions and emit solid film exhibited fluorescence in 541 nm. Furthermore, the result of ionization potential of dye demonstrated value of 5.89 eV. The PLQY of dye in solid film was high value rather than to solutions, therefore we investigated aggregation tests and the

dye was aggregation induced emission (AIE). Moreover the  $\tau$  of PL Decay spectra of dye was 9.11 ns. The result of absorption spectra showed shift to high wavelength in solid state film rather than to solution that it's concerning to the j aggregation of dye.

#### ACKNOWLEDGEMENT

This research was supported by Research Center of Materials Engineering, IAUN no 1398/2146

#### REFERENCES

[1]. Y. Danyliv, R. Lytvyn, D. Volyniuk, O. Bezvikonnyi, I. Hladka, J.V. Grazulevicius. Derivatives of carbazole and chloropyridine

exhibiting aggregation induced emission enhancement and deep-blue delayed fluorescence, *Dye Pigment*. 149 (2018) 588–596. <https://doi.org/10.1016/j.dyepig.2017.11.027>

[2]. L. Duan, J. Qiao, Y. Sun, Y. Qiu. Strategies to design bipolar small molecules for OLEDs: donor-acceptor structure and non-donor-acceptor structure. *Adv. Mat.* 23 (2011) 1137–44. <https://doi.org/10.1002/adma.201003816>

[3]. Tang J, Hua J, Wu W, Li J, Jin Z, Long Y, et al. New starburst sensitizer with carbazole antennas for efficient and stable dye-sensitized solar cells. *Energy Environ Sci* 3 (2010) 1736–45. <https://doi.org/10.1039/C0EE00008F>

[4]. Jiao C-X, Shen Q, Huan S-Y, Shen G-L, Yu R-Q. Conjugated carbazole dimer as fluorescence carrier for preparation of iodine sensitive chemical sensor. *Chim. Acta* 528 (2005) 229–34. <http://dx.doi.org/10.1016/j.aca.2004.04.061>

[5]. Sato K, Shizu K, Yoshimura K, Kawada A, Miyazaki H, Adachi C. Organic luminescent molecule with energetically equivalent singlet and triplet excited states for organic light-emitting diodes. *Phys. Rev. Lett.* 110 (2013) 247401 (1–5). <https://doi.org/10.1103/PhysRevLett.110.247401>

[6]. A. Mishra, P. Bauerle. Small molecule organic semiconductors on the move: promises for future solar energy technology. *Angew. Chem. Int. Ed.* 51 (2012) 2020. <https://doi.org/10.1002/anie.201102326>

[7]. S. M. Feldt, E. A. Gibson, E. Gabriellson, L. Sun, G. Boschloo and A. Hagfeldt. Design of Organic Dyes and Cobalt Polypyridine Redox Mediators for High-Efficiency Dye-Sensitized Solar Cells. *J. Am. Chem. Soc.* 132 (2010) 16714–16724. <https://doi.org/10.1021/ja1088869>

[8]. Y. Bai, J. Zhang, D. Zhou, Y. Wang, M. Zhang and P. Wang. Engineering Organic Sensitizers for Iodine-Free Dye-Sensitized Solar Cells: Red-Shifted Current Response Concomitant with Attenuated Charge Recombination *J. Am. Chem. Soc.* 133 (2011) 11442–11445. <https://doi.org/10.1021/ja203708k>

[9]. M. Wang, C. Grätzel, S. M. Zakeeruddin and M. Grätzel. Recent developments in redox electrolytes for dye-sensitized solar cells. *Energy Environ. Sci.* 5 (2012) 9394–9405. <https://doi.org/10.1039/C2EE23081J>

[10]. Z. H. Wang, M. Liang, L. Wang, Y. Hao, C. Wang, Z. Sun and S. Xue. New triphenylamine organic dyes containing dithienopyrrole (DTP) units for iodine-free dye-sensitized solar cells. *Chem. Commun.* 49 (2013) 5748–5750. <https://doi.org/10.1039/C3CC42121J>

[11]. W. Zhu, Y. Wu, S. Wang, W. Li, X. Li, J. Chen, Z. S. Wang, H. Tian. Organic D-A- $\pi$ -A Solar Cell Sensitizers with Improved Stability and Spectral Response. *Adv. Funct. Mater.* 21 (2011) 756–763. <https://doi.org/10.1002/adfm.201001801>

[12]. X. F. Lu, Q. Y. Feng, T. Lan, G. Zhou, Z. S. Wang. Molecular Engineering of Quinoxaline-Based Organic Sensitizers for Highly Efficient and Stable Dye-Sensitized Solar Cells. *Chem. Mater.* 24 (2012) 3179–3187. <https://doi.org/10.1021/cm301520z>

[13]. Y. Ooyama, T. Nagano, S. Inoue, I. Imae, K. Komaguchi, J. Ohshita and Y. Harima. Dye-sensitized solar cells based on donor- $\pi$ -acceptor fluorescent dyes with a pyridine ring as an electron-withdrawing-injecting anchoring group. *Chem. Eur. J.* 17 (2011) 14837–43. <https://doi.org/10.1002/chem.201101923>

[14]. H. Tan, C. Pan, G. Wang, Y. Wu, Y. Zhang, Y. Zou, G. Yu, M. Zhang. Phenoxazine-based organic dyes with different chromophores for dye-sensitized solar cells. *Org. Electron.* 14 (2013) 2795–2801. <http://dx.doi.org/10.1016/j.orgel.2013.07.008>

[15]. T.Y. Wu, M.H. Tsao, F.J. Chen, S.G. Su, C.W. Chang, H.P. Wang, Y.C. Lin, I.W. Sun. Synthesis and characterization of three organic dyes with various donors and rhodanine ring acceptor for use in dye-sensitized solar cells. *J. Iran. Chem. Soc.* 7 (2010) 707–720. <http://dx.doi.org/10.1007/BF03246061>

[15]. M. Akhtaruzzaman, A. Islam, A. El-Shafei, N. Asao, T. Jin, L. Han, K.A. Alamry, S.A. Kosa, A.M. Asiri, Y. Yamamoto. Structure-property relationship of different electron donors: Novel organic sensitizers based on fused dithienothiophene  $\pi$ -conjugated linker for high efficiency dye-sensitized solar cells. *Tetrahedron* 69 (2013) 3444–3450. <https://doi.org/10.1016/j.tet.2013.02.058>

[16]. L.L. Tan, L.J. Xie, Y. Shen, J.M. Liu, L.M. Xiao, D.B. Kuang,

- C.Y. Su. Novel organic dyes incorporating a carbazole or dendritic 3,6-diiodocarbazole unit for efficient dye-sensitized solar cells. *Dyes Pig* 100 (2014) 269-277. <https://doi.org/10.1016/j.dyepig.2013.09.025>
- [17]. Z. Wan, C. Jia, Y. Duan, X. Chen, Y. Lin, Y. Shi. Novel organic dye employing dithiafulvenyl-substituted arylamine hybrid donor unit for dye-sensitized solar cells. *Org Electron* 14 (2013) 2132-2138. <https://doi.org/10.1016/j.orgel.2013.05.011>
- [18]. C. Paul, A. Pockett, G. Kociok-Köhn, P.J. Cameron, S.E. Lewis. Azulene – Thiophene – Cyanoacrylic acid dyes with donor- $\pi$ -acceptor structures. Synthesis, characterisation and evaluation in dye-sensitized solar cells. 74 (2018) 2775-2786. <https://doi.org/10.1016/j.tet.2018.04.043>
- [19]. A. Dehno Khalaji, M. Mogheiseh, V. Eigner, M. Dusek, T.J. Chow, E. Maddahi. Synthesis, characterization and crystal structures of new organic compounds containing cyanoacrylic acid. *Journal of Molecular Structure*. 1098 (2015) 318-323. <https://doi.org/10.1016/j.molstruc.2015.05.033>
- [20]. X. Qian, R. Yan, Y. Hang, Y. Lv, L. Zheng, C. Xu, L. Hou. Indeno[1,2-b]indole-based organic dyes with different acceptor groups for dye-sensitized solar cells. *Dyes and Pigments* 139 (2017) 274-282. <https://doi.org/10.1016/j.dyepig.2016.12.028>
- [21]. T.B. Fleetham, L. Huang, K. Klimes, J. Brooks, Jian Li. Tetradentate Pt(II) Complexes with 6-Membered Chelate Rings: A New Route for Stable and Efficient Blue Organic Light Emitting Diodes. *Chem. Mater* 28 (2016) 3276-3282. <https://doi.org/10.1021/acs.chemmater.5b04957>
- [22]. M. Hosseini, S. Rouhani, K. Gharanjig, Extraction and application of natural pigments for fabrication of green dye-sensitized solar cells, *Opto-Electronic Review*. 26 (2018) 165-171. <http://dx.doi.org/10.1016/j.opelre.2018.04.004>
- [23]. E. Miyamoto, Y. Yamaguchi, M. Yokoyama. Ionization potential of organic pigment film by atmospheric photoelectron emission analysis, *Electrophotography* 28 (1989) 364-370. <http://doi.org/10.11370/isjsep.28.364>
- [24]. N.A. Kukhta, D. Volyniuk, L. Peculyte, J. Ostrauskaite, G. Juska, J.V. Grazulevicius. Structure-property relationships of star-shaped blue-emitting charge-transporting 1,3,5-triphenylbenzene derivatives, *Dye Pigment*. 117 (2015) 122-32. <http://dx.doi.org/10.1016/j.dyepig.2015.02.013>
- [25]. Frisch MJ, Trucks GW, Schlegel HB, Scuseria GE, Robb MA, Cheeseman JR, et al. Gaussian 09, revision D.01. Wallingford CT: Gaussian, Inc (2016).
- [26]. Allouche AR. Gabedit - a graphical user interface for computational chemistry softwares. *J Comput Chem* 32 (2011) 174-82. <http://dx.doi.org/10.1002/jcc.21600>
- [27]. P. Politzer, F. Abu-Awwad, A comparative analysis of Hartree-Fock and Kohn-Sham orbital energies. *Theor Chim Acta* 99 (1998) 83-87. <https://doi.org/10.1007/s002140050307>
- [28]. K. Wu, Z. Wang, L. Zhan, C. Zhong, S. Gong, G. Xie, C. Yang. Realizing Highly Efficient Solution-Processed Homo Junction-Like Sky-Blue OLEDs by Using Thermally Activated Delayed Fluorescent Emitters Featuring an Aggregation-Induced Emission Property. *J Phys Chem Lett* 9 (2018) 1547-1553. <https://doi.org/10.1021/acs.jpclett.8b00344>
- [29]. B.W. Andrade, S. Datta, S. Forrest, P. Djurovich, E. Polikarpov, M.E. Thompson. Relationship between the ionization and oxidation potentials of molecular organic semiconductors, *Organic Electronics* 6 (2005) 11-20. <https://doi.org/10.1016/j.orgel.2005.01.002>
- [30]. Karpicz R, Puzinas S, Krotkus S, Kazlauskas K, Jursenas S, Grazulevicius JV, et al. Impact of intramolecular twisting and exciton migration on emission efficiency of multifunctional fluorene-benzothiadiazole-carbazole compounds. *J Chem Phys* 134 (2011) 204508.1-9. <http://doi.org/10.1063/1.3594047>
- [31]. Youn S, Yasuda T, Nomura H, Adachi C. High Efficiency Organic Light-Emitting Diodes Utilizing Thermally Activated Delayed Fluorescence from Triazine-Based Donor-Acceptor Hybrid Molecules. *Appl Phys Lett* 101 (2012) 093306. <http://doi.org/10.1063/1.4749285>
- [32]. Santos PL, Ward JS, Data P, Batsanov AS, Bryce MR, Dias FB, Monkman AP. Engineering the Singlet-triplet Energy Splitting in a TADF Molecule. *J Mater Chem C* 4 (2016) 3815-3824. <http://doi.org/10.1039/C5TC03849A>
- [33]. Dias FB, Santos J, Graves D, Data P, Nobuyasu RS, Fox, MA, Batsanov AS, Palmeira T, Berberan MN, Bryce MR, Monkman AP. The Role of Local Triplet Excited States in Thermally-Activated Delayed Fluorescence: Photophysics and Devices. *Adv Sci* 3 (2016) 1600080. <http://doi.org/10.1002/advs.201600080>
- [34]. Li W, Liu D, Shen F, et al. A Twisting Donor-Acceptor Molecule with an Intercrossed Excited State for Highly Efficient, Deep-Blue Electroluminescence. *Adv Funct Mater* 22 (2012) 2797-2803. <http://doi.org/10.1002/adfm.201200116>
- [35]. Li W, Pan Y, Xiao R, et al. Employing ~100% Excitons in OLEDs by Utilizing a Fluorescent Molecule with Hybridized Local and Charge-Transfer Excited State. *Adv Funct Mater* 24 (2014) 1609-1614. <http://doi.org/10.1002/adfm.201301750>
- [36]. Etherington MK, Franchello F, Gibson J, Northey T, Santos J, Ward JS, Data P, Kurowska, A, Santos PL, Graves DR et al. Regio- and Conformational Isomerisation Critical to Design of Efficient Thermally-Activated Delayed Fluorescence Emitters. *Nature Communications* 8 (2017) 14987. <http://doi.org/10.1038/ncomms14987>
- [37]. Tanaka H, Shizu K, Nakanotani H, Adachi C. Dual Intramolecular Charge-Transfer Fluorescence Derived from a Phenothiazine-Triphenyltriazine Derivative. *J Phys Chem C* 118 (2014) 15985-15994. <http://doi.org/10.1021/jp501017f>
- [38]. Okazaki M, Takeda Y, Data P, Pander P, Higginbotham H, Monkman AP, Minakata S. Thermally Activated Delayed Fluorescent Phenothiazine-Dibenzo[a,j]phenazine Phenothiazine Triads Exhibiting Tricolor-Changing Mechanochromic Luminescence. *Chem Sci* 8 (2017) 2677-2686. <http://doi.org/10.1039/C6SC04863C>
- [39]. Ellinger S, Graham KR, Shi P, Farley RT, Steckler T T, Brookins RN, Taraneke P, Schanze, Mei J, Padilha LA, Ensley T R, Hu H, Webster S, Hagan DJ, Van Stryland EW, Schanze KS, K. S. Reynolds JR. Donor-Acceptor-Donor-based  $\pi$ -Conjugated Oligomers for Nonlinear Optical and Near-IR Emission. *Chem Mater* 23 (2011) 3805-17. <http://doi.org/10.1021/cm201424a>
- [40]. Du X, Qi J, Zhang Z, Ma D, Wang Z. Efficient Non-doped Near Infrared Organic Light-Emitting Devices Based on Fluorophores with Aggregation-Induced Emission Enhancement. *Chem Mater* 24 (2012) 2178-2185. <http://doi.org/10.1021/cm3008733>
- [42]. Zh Yang, Zh Mao, Zo Xie, Yi Zhang, S Liu, J Zhao, J Xu, Zh Chi, M Aldredb. Recent advances in organic thermally activated delayed fluorescence. *Materials Chem. Soc. Rev* 46 (2017) 915-1016. <http://doi.org/10.1039/c6cs00368k>
- [43]. Hoffmann ST, Schre'gel P, Rothmann M, Albuquerque RQ, Strohmriegl P, Ko'hler A. Triplet excimer emission in a series of 4,4'-bis( N -carbazolyl)-2,2'-biphenyl derivatives. *J Phys Chem B* 115 (2011) 414-21. <http://dx.doi.org/10.1021/jp107408e>
- [44]. G.G. Kaminskiene, D. Volyniuk V. Mimaite, O. Bezikonny, A. Bucinskas, G. Bagdziunas, J.V. Grazulevicius. Aggregation-Enhanced Emission and Thermally Activated Delayed Fluorescence of Derivatives of 9-Phenyl-9H-Carbazole: Effects of Methoxy and tert-Butyl Substituents. *Chemistry European Journal* 24 (2018) 9581-9591. <https://doi.org/10.1002/chem.201800822>
- [45]. Zassowski P, Ledwon P, Kurowska A, Herman AP, Jarosz T, Lapkowski M, et al. Efficient synthesis and structural effects of ambipolar carbazole derivatives. *Synth Met* 223 (2017) 1-11. <http://dx.doi.org/10.1016/j.synthmet.2016.11.015>
- [46]. Stockmann A, Kurzawa J, Fritz N, Acar N, Schneider S, Daub J, Engl R, Clark T. Conformational control of photoinduced charge separation within phenothiazine-pyrene dyads. *J Phys Chem A* 106 (2002) 7958-7970. <http://doi.org/10.1021/jp0142987>
- [47]. Chan C, Lam Ja, Zhao Zu, Chen Sh, Lu Pi, Sung He, Kwok Ho,



- Ma Yu, Williams Ian, Tang Be. Aggregation-induced emission, mechanochromism and blue electroluminescence of carbazole and triphenylamine-substituted ethenes. *J Mater Chem C* 2 (2014) 4320–4327. <http://doi.org/10.1039/C4TC00097H>
- [48]. Tanaka H, Shizu K, Nakanotani H, Adachi C. Dual intramolecular charge-transfer fluorescence derived from a phenothiazine-triphenyltriazine derivative. *J Phys Chem C* 118 (2014) 15985–15994. <http://doi.org/10.1021/jp501017f>
- [49]. A. Tomkeviciene, J. Sutaite, D. Volyniuk, N. Kostiv, G. Simkus, V. Mimaite.; JV. Grazulevicius, Aggregation-Induced Emission Enhancement in Charge-Transporting Derivatives of Carbazole and Tetra(tri)phenylethylene, *Dyes Pigm* 140 (2017) 363–374. <http://dx.doi.org/10.1016%2Fj.dyepig.2017.01.056>.